Contents list available at IJRED website

International Journal of Renewable Energy Development

Journal homepage: https://ijred.undip.ac.id

Research Article

# Unveiling frequency-dependent dielectric behavior of cellulose-based polymer electrolyte at various temperature and salt concentration

Christin Rina Ratri[1,2*], Qolby Sabrina[2], Titik Lestariningsih[2], Adam Febriyanto Nugraha[1,3], Sotya Astutiningsih[1], Mochamad Chalid[1]

[1]*Department of Metallurgical and Materials Engineering, Faculty of Engineering, Universitas Indonesia, Kampus Baru UI Depok, Jawa Barat, 16424, Indonesia*

[2]*Research Center of Advanced Materials, National Research and Innovation Agency (BRIN), KST BJ. Habibie, Gd. 440-441, Tangerang Selatan, Banten, Indonesia.*

[3]*Asosiasi Peneliti Indonesia di Korea (APIK), Seoul, 07342, South Korea*

**Abstract**. Dielectric behavior of cellulose-based polymer electrolyte was studied at various temperature and salt concentration. A polymer electrolyte membrane based on cellulose acetate (CA) as the polymer host and LiClO4 as the dopant salt was fabricated using the solution casting technique. The dopant salt concentration was varied as 0.3, 0.5, 0.67, and 1M. Dielectric relaxation spectroscopy characterization were performed using potentiostat at frequency ranging from 0.1 Hz to 1 MHz. Measurements were performed by sandwiching the membrane between stainless steel plates. The ionic conductivity was then calculated based on the Cole–Cole plot obtained from the impedance measurement. It was found that sample 1 M had the highest ionic conductivity at high frequencies. However, the frequency-dependent conductance plot showed that the ionic conductivity of the 1 M sample significantly decreased at low frequencies, i.e. from $3.41\times10^{-5}$ S/cm at 1 MHz to $1.9\times10^{-8}$ S/cm at 0.1 Hz. Other samples did not experience this phenomenon, including those with a Celgard© commercial membrane to represent commercial Li-ion batteries. This is caused by excess charge accumulation, leading to a high concentration of immobile charge carriers, which reduces the available free volume surrounding the polymer chain. This resulted in a significant decrease in ionic conductivity at low frequencies. Temperature variation was also performed on the conductivity measurement at 30-70 °C. Temperature variation showed more predictable behavior, where increasing the temperature activated charge carriers and enhanced ionic conductivity, from $1.81\times10^{-5}$ S/cm at room temperature to $9.04\times10^{-5}$ at 70°C. Sweeping across the frequency range results in a consistent sequence of ionic conductivities among the samples at various temperatures. This work is beneficial for evaluating a biomass-based polymer electrolyte complex in a Li-ion battery environment. Feasibility studies can be performed at various concentrations and temperatures to determine the optimal level of dopant salt input across a broad frequency range.

**Keywords:** cellulose acetate, polymer electrolyte, ionic conductivity, dielectric properties



Received: 18th March 2023; Revised: 2nd June 2023; Accepted: 20th June 2023; Available online: 30th June 2023

## 1. Introduction

Since its commercialization in 1991 by Sony, lithium ion batteries (LIBs) have emerged as one of the most widely commercialized energy storage systems, as they can be utilized for portable devices, large-scale power sources, and electric vehicles. Along with the positive and negative electrodes, the separator and electrolyte pair play an important role, as they separate the two electrodes, preventing short circuits while allowing efficient diffusion of lithium ions between them. Therefore, an ideal separator should be composed of thin and porous electrical insulators and ionic-conducting materials. The separator must also ensure rapid diffusion of ions between the electrodes, easy wetting by liquid electrolytes, and resistance to electrochemical interactions. These requirements are necessary to protect the battery from the possibility of thermal runaway (Zalosh *et al.*, 2021). The separator-electrolyte pair in conventional batteries is usually a polymer separator sheet immersed in a liquid electrolyte, that is, salts dissolved in a mixture of one or more solvents, ensuring rapid diffusion of ions across the electrode/electrolyte interface and separator. Although high ionic conductivities can be achieved, the use of liquid electrolytes carries serious safety risks associated with possible electrolyte leakage, which can cause the battery to become flammable and even explode. To avoid these undesirable events, solid polymer electrolytes (SPEs) have been developed, in which a separator sheet also functions as an electrolyte, so that electrolytes in liquid form are no longer needed (Maia *et al.*, 2022).

It is also necessary to produce battery separators using renewable natural resources as raw materials, considering that commercial LIBs separators are currently made from petroleum-based polymers, namely, polypropylene or trilayer polypropylene/polyethylene/polypropylene (X. Zhao *et al.*, 2021). Renewable natural resource-based polymers (biopolymers) have the greatest potential for development into

* Corresponding author
Email: christin.rina.ratri@brin.go.id (C.R. Ratri)

https://doi.org/10.14710/ijred.2023.53103
ISSN: 2252-4940/© 2023.The Author(s). Published by CBIORE

sustainable, non-toxic, and biodegradable LIBs separators (Galiano *et al*., 2018).

Biopolymers are generally obtained from renewable sources (plants, animals, or microorganisms). Unfortunately, competition for food production has shifted the focus of biopolymer research to biomass from non-edible plants or agricultural/plantation waste (Awang *et al., 2021;* Sampath *et al*., 2016). Among the various biopolymer feedstocks, cellulose has emerged as the most sustainable material to replace conventional petropolymer separators owing to its unique properties, namely, hydrophilicity, low density, excellent mechanical strength, and versatile functionality (Lizundia *et al*., 2020). Cellulose is the most abundant raw material for biopolymers and can be extracted from agricultural/plantation waste to avoid triggering competition with food production. The utilization of cellulose as a raw material for biopolymers will help reduce the scarcity of non-renewable resources, while reducing the accumulation of plastic waste because of its biodegradable nature (Deng *et al*., 2019).

Native cellulose possesses a hydroxyl group as the terminal functional group. Tunable properties can be achieved by substituting hydroxyl groups with cellulose derivatives containing the intended groups. For example, modification of cellulose into a thermoplastic cellulose acetate polymer is carried out by adding acetic acid and replacing the hydroxyl group with acetate. The loss of some hydroxyl groups reduces the hygroscopic nature of the membrane, thereby reducing the potential for degradation of the electrode material and a decrease in the capacity of the battery cells due to ambient air humidity (Yang *et al*., 2010). This is an important issue to consider in LIBs production in relatively humid regions such as Indonesia. Thus, cellulose acetate is widely used as a raw material in various membrane applications, such as reverse osmosis, ultrafiltration, microfiltration, adsorption membranes, gas separation, and ion exchange membranes (Chaurasia *et al*., 2022; Hu *et al*., 2020; Wang *et al*., 2019).

The utilization of cellulose acetate as a standalone polymer matrix in LIBs SPE systems still needs to be improved, as it exhibits several weaknesses, including low thermal stability and relatively high glass transition temperatures. The addition of an electrolyte salt is expected to produce a higher charge carrier concentration, thereby boosting the ionic conductivity of the polymer electrolyte system. Various salts have been used in CA-based polymer electrolyte systems such as $LiClO_4$, LiTFSI, $NH_4SCN$, and $NH_4I$ (Monisha *et al*., 2016; Razalli *et al*., 2015; Sudiarti *et al*., 2017). These experiments agree that increasing the salt concentration improves the ionic conductivity to a maximum; afterwards, it tends to form aggregates that hinder ionic dissociation, thereby decreasing its conductivity (Aziz *et al*., 2017). Research on cellulose acetate (CA)-based solid polymer electrolytes using $LiClO_4$, such as the work by Arcana et al., has made way for cellulose-based membranes for Li-ion battery applications (Arcana *et al*., 2014; Sudiarti *et al*., 2017). Thus far, experiments on CA-$LiClO_4$ solid polymer electrolyte membranes have calculated the ionic conductivity at different concentrations and temperatures without further exploring the frequency-dependent behavior of ionic species in the polymer electrolyte membrane.

Dielectric properties have been widely studied to assess the general performance of SPEs in terms of their ionic conductivity. The ionic conductivity, as we know, is calculated from the impedance value resulting from a certain applied frequency. In this work, we experimented using various dopant salt concentrations as well as measurement temperatures and analyzed the dielectric properties to obtain a deeper understanding of the behavior of polymer electrolyte complexes over a wide range of frequencies.

## 2. Experimental methods

### *2.1. Materials*

Cellulose acetate (CA) (Sigma Aldrich, 30 kDa) was used without further purification. The lithium perchlorate ($LiClO_4$) electrolyte salt (Sigma Aldrich) was heated at 105°C for 24 h prior to the experiment to remove trace moisture. The solvent N-methyl pyrrolidone (NMP) (Merck, analytical grade) was used throughout the experiment.

Membrane fabrication

The CA membrane was fabricated using a solution casting technique. Cellulose acetate was dissolved in the NMP solvent using a magnetic stirrer on a hot plate set at 50°C and stirred at 500 rpm until a clear solution was formed, indicating a homogeneous mixture. The resulting slurry was poured into a Petri dish and dried in a vacuum oven at 70°C for 48 h. The freestanding CA membrane was then peeled off from the Petri dish and stored in a dry box prior to activation and measurement.

### *2.2. Membrane activation*

To activate the CA membrane as a solid polymer electrolyte, $LiClO_4$ salt with various concentrations (0.3, 0.5, 0.67, and 1 M) were dissolved in ethanol at room temperature. The CA membrane was cut into small discs (19 mm diameter) and soaked in an electrolyte salt solution for two hours. For comparison with commercial cells, Celgard ® membranes were also prepared using a similar treatment with 1 M salt concentration.

### *2.3. Membrane characterization*

The dielectric properties of the polymer electrolyte membranes were observed using Electrochemical Impedance spectroscopy (EIS). The immersed membrane was sandwiched between two blocking electrodes made of stainless steel (SS) plates, forming SS/membrane/SS configurations, and assembled into a

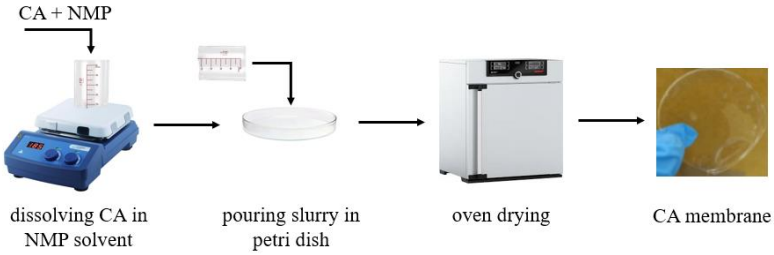


**Fig 1.** Schematic representation of CA membrane fabrication

CR2032 battery coin cell. The battery cell was measured using a Metrohm Autolab potentiostat with an applied frequency range of 0.1 to $10^6$ Hz. Temperature variation of 30–70 °C was also performed to observe the dielectric behavior of the solid polymer electrolyte.

The ionic conductivity, σ, was calculated using the following equation:

$$\sigma = t/R_bA, \quad (1)$$

where A is the contact area of the polymer electrolyte membrane, t is the membrane thickness, and $R_b$ is the bulk resistance obtained from the intercept of the real impedance axis. The complex impedance Z* can be expressed using the following equation:

$$Z^* = Z' + iZ'', \quad (2)$$

where Z' is the real impedance and Z'' is the imaginary impedance. Using these values and the frequency variable, the dielectric constant ε' and dielectric loss ε" as well as real and imaginary electrical modulus (M' and M," respectively) were calculated using the following equations:

$$\varepsilon'(\omega) = Z''/[\omega C_0 (Z'^2 + Z''^2)], \quad (3)$$

$$\varepsilon''(\omega) = Z'/[\omega C_0 (Z'^2 + Z''^2)], \quad (4)$$

$$M'(\omega) = \varepsilon'/(\varepsilon'^2 + \varepsilon''^2), \quad (5)$$

$$M''(\omega) = \varepsilon''/(\varepsilon'^2 + \varepsilon''^2), \quad (6)$$

where the angular frequency ω is 2πf, f is the frequency in Hz, and $C_0 = \varepsilon_0 A/t$, where $\varepsilon_0$ is the vacuum space permittivity.

Functional groups and their interactions within the polymer electrolyte membranes were observed using FT-IR Thermo Scientific Nicolet iS10 in ATR mode, set at a wavenumber range of 4000-800 $cm^{-1}$ with scan resolution of 2 $cm^{-1}$.

## 3. Results and discussions

### *3.1 FTIR spectroscopy*

The complex formation of the CA membrane was demonstrated using FTIR spectroscopy. As shown in Figure 2, the band at approximately 3468 $cm^{-1}$ is attributed to the O-H stretching of pure CA. The peak at 1742 $cm^{-1}$ is attributed to the aldehyde carbonyl group C=O stretching. C-H bending in pure CA alkanes is responsible for the medium-intensity peak at 1368 $cm^{-1}$ (Das et al., 2014). The absorption peak at 1218 $cm^{-1}$ is attributed to the ester group C-O stretching. The peak observed at 1031 $cm^{-1}$ was attributed to the C-O-C stretching of a pyrose ring, and the medium-intensity peak at 900 $cm^{-1}$ was attributed to the pure CA O-H bending vibrational mode (Ramesh *et al.*, 2013). Compared to the FT-IR spectra of the CA powder (dotted line), these fingerprint peaks show that during the membrane fabrication process, no modification occurred in terms of the chemical bonds.

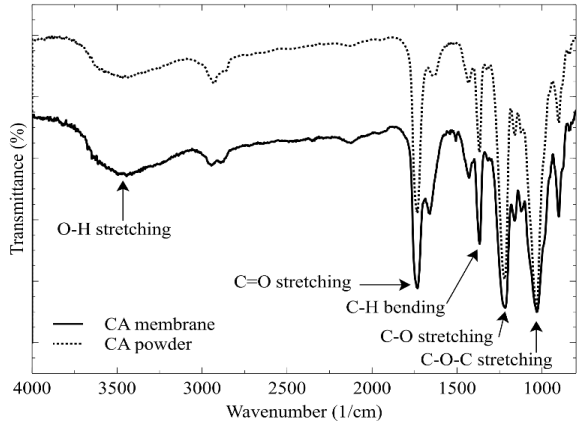


**Fig 2**. FT-IR transmission spectra of CA membrane and powder

### *3.2 Salt concentration-dependent conductivity*

Cole-Cole plots from EIS measurements of polymer electrolyte membranes using various $LiClO_4$ salt concentrations are presented in Figure 3. Typically, impedance plots reveal low-frequency regions with inclined spikes, and high-frequency regions with semicircles (Fernández-Sánchez *et al.* 2005). The spike region indicates electrical double-layer capacitance formation due to the accumulation of free charges across the interface facing the polymer electrolyte membrane and the electrode surface. The semicircle or arc region can be assigned to the charge transfer process around the interfaces in the cell (He *et al.*, 2017). The disappearance of the entire or part of the semicircle in the high-frequency region suggests that the ionic conductivity of the polymer electrolyte membrane results from ion migration (Arya & Sharma, 2018). The ionic conductivity was calculated using Equation 1. The ionic conductivities of CA-$LiClO_4$ at various concentrations are listed in Table 1.

It was revealed that CA 1 M exhibits a maximum ionic conductivity of $3.41\times10^{-5}$ S/cm at room temperature. A high number of charge carriers improved the ionic mobility to generate a feasible performance for the lithium-ion battery. This is in agreement with the fact that the ionic conductivity of an electrolyte system depends on the charge carrier concentration, according to the following equation:

$$\sigma = n \times e \times u, \quad (7)$$

where n is the charge-carrier concentration, e is the charge of the mobile carrier, and u is the charge-carrier mobility (Alipoori *et al.*, 2021).

Nevertheless, increasing the salt concentration is not always advantageous; a high salt concentration could result in aggregation and association that hinders ionic mobility (Y. Zhao *et al.*, 2018). For comparison, a Celgard separator immersed in 1 M $LiClO_4$ (denoted as Celgard 1 M) was also assembled with a similar configuration and characterization parameters. The Celgard 1 M sample represents a conventional battery for commercial use, which employs a Celgard separator immersed in a liquid electrolyte. Impedance measurements showed that CA 1 M exhibited higher conductivity ($3.41\times10^{-5}$ S/cm) than Celgard 1 M ($1.49\times10^{-5}$ S/cm). This suggests that cellulose-based polymer electrolytes can potentially substitute

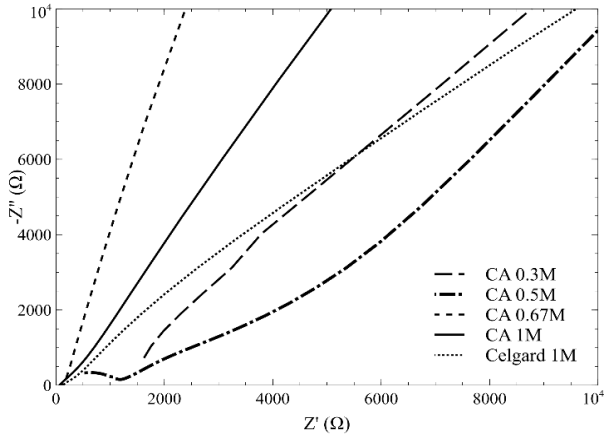


**Fig 3**. Cole-cole plot of CA SPE with different salt concentration

**Table 1**
Room temperature ionic conductivity of CA membranes at different concentration and Celgard 1M

| Sample | Ionic conductivity, S/cm | |
|---|---|---|
| | 0.1 Hz | 1 MHz |
| CA 0.3 M | $8.77\times10^{-9}$ | $5.82\times10^{-6}$ |
| CA 0.5 M | $1.14\times10^{-7}$ | $4.08\times10^{-6}$ |
| CA 0.67 M | $2.7\times10^{-7}$ | $2.65\times10^{-5}$ |
| CA 1 M | $1.9\times10^{-8}$ | $3.41\times10^{-5}$ |
| Celgard 1M | $1.23\times10^{-9}$ | $1.38\times10^{-6}$ |

**Table 2**
CA-$LiClO_4$ 1M ionic conductivity at different temperature

| Temperature (°C) | Ionic conductivity (S/cm) |
|---|---|
| 30 | $1.81\times10^{-5}$ |
| 40 | $2.33\times10^{-5}$ |
| 50 | $3.84\times10^{-5}$ |
| 60 | $6.22\times10^{-5}$ |
| 70 | $9.04\times10^{-5}$ |

commercial polyolefin separators for lithium-ion battery applications.

Impedance spectroscopy was used to test the ionic conductivity of polymer electrolytes at temperatures between 30°C and 70°C. These findings suggested that the polymer matrix did not undergo dynamic structural changes. The ionic conductivities of the CA polymer electrolyte membranes at various temperatures are listed in Table 2.

It can be seen from Table 2 that higher temperatures result in higher ionic conductivities. Increasing the temperature within the membrane caused the polymer to expand, and consequently, more free volume was generated. This leads to enhanced polymer segmental mobility and ionic conductivity. The behavior of conductivity variation in polymer electrolytes conforms to the Arrhenius model, which characterizes transport properties within a viscous polymer matrix (Polu *et al*., 2015). The phenomenon of enhanced conductivity with increasing temperature can be explained as a process of hopping between coordinating sites, local structural relaxation, and segmental motions of polymer electrolyte complexes, as described in reference. With increasing temperature, the polymer chain experiences accelerated internal modes, leading to bond rotations that result in segmental motion. As a result, there is a preference for ion movement both within and between polymer chains, leading to an increase in the conductivity of the polymer electrolyte (Malathi *et al*., 2010).

### *3.3 Conductance spectra*

The frequency-dependent conductance spectra of the CA SPEs at various salt concentrations and temperatures are shown in Figure 4(a) and (b), respectively. These spectra can be divided into two regions: a low-frequency dispersive region representing the electrode-electrolyte interface interaction and a higher frequency plateau representing DC conductivity. With decreasing frequency, free charge accumulates at the electrode-electrolyte interface, resulting in a decrease in mobile ions. This means that a lower conductivity is obtained in the lower frequency region (Aziz *et al*., 2017; Razalli *et al*., 2015). The ionic conductivities of the polymer electrolyte samples at the lowest and highest frequencies are presented in Table 1.

At high frequencies of approximately 100 kHz to 1 MHz, they follow the notion that a higher salt concentration results in higher ionic conductivity owing to the increasing number of charge carriers, as presented in Figure 4 and Table 1. However, as the frequency was lower than 100 kHz, it can be observed that the ionic conductivity of both samples CA and Celgard 1 M decreased significantly with steeper slopes compared to samples with lower concentration (0.3 M, 0.5, and 0.67 M). At final 0.1 Hz frequency, CA 1 M ionic conductivity is found to be lower than CA 0.67 M and CA 0.5 M. Ionic conductivity of Celgard 1 M was higher than CA 0.5 M at 1 MHz frequency, but at 0.1 Hz it shows the opposite result.

This behavior can be explained as follows. At high frequencies, a high number of charge carriers as well as the high mobility of these ions are observed, resulting in the highest ionic conductivity, as seen in the conductance spectra and the Cole–Cole plot. However, at lower frequencies, excessive charge accumulation occurs, and a large amount of immobile charge carriers results in less free volume around the polymer chain (Arya & Sharma, 2017). Consequently, the ionic conductivity drops significantly, as seen in the conductance spectra of sample 1 M. High salt concentrations also promote ion pairing, which leads to a lower ionic conductivity (Karan *et al*., 2008).

In this study, Celgard 1 M was utilized as a representative commercial Li-ion battery currently available in the market to highlight the potential of using CA as a substitute. The ionic conductivity of Celgard 1 M was lower than that of CA 1 M in all frequency ranges. This is in agreement with the research performed by Gou and Zhao (Gou *et al*., 2020; X. Zhao *et al*., 2021). It is assumed that cellulose-based polymer electrolytes

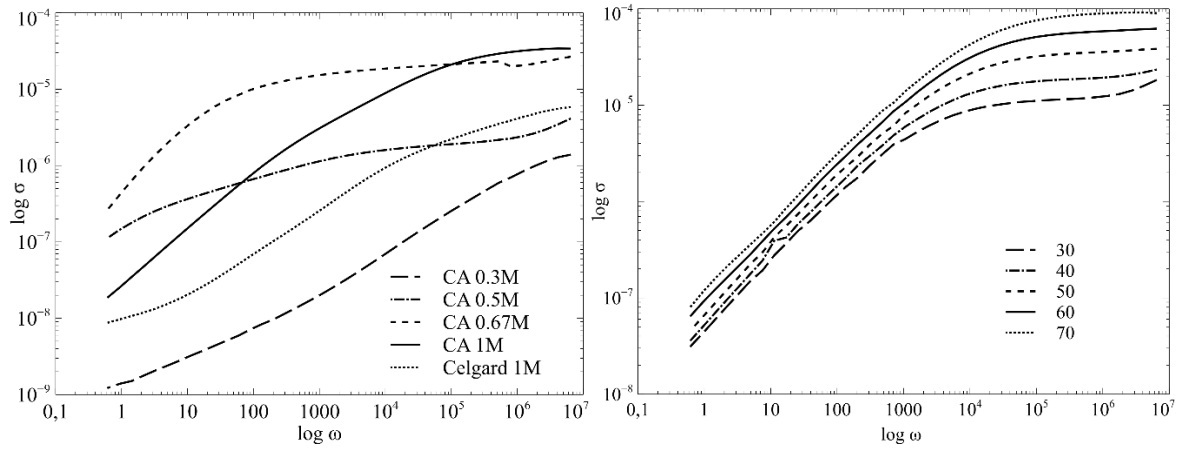


**Fig 4.** Conductance spectra of CA SPEs at different (a) salt concentration and (b) temperature

exhibit superior electrochemical performance compared to commercial Li-ion batteries with Celgard© separators.

Temperature variation has shown a more predictable behavior. Increasing the temperature led to an increase in the number of thermally activated charge carriers. This results in a higher free volume and vacant sites for ionic motion, which enhances the ionic conductivity (Karthika *et al*., 2017). The drop in viscosity and subsequent increase in chain flexibility may be the cause of the conductivity increase with temperature. Polymer segmental motion promotes translational ionic motion. The conductivity dispersion is observed to be less significant at lower temperatures, and as the temperature rises, the dispersion becomes more prominent in the higher frequency region. In other words, as the temperature increases, the bulk relaxation changes to higher frequencies (Tamilselvi & Hema, 2014).

### *3.4 Dielectric analysis*

Frequency (f) dependency of the dielectric constant and dielectric loss of CA polymer electrolyte membrane at different salt concentration and temperature is shown in Figure 5. The real and imaginary components of the complex permittivity ε*, which can be expressed by the following relation, can be used to characterize the dielectric behavior of any polymeric system:

$$\varepsilon^* = \varepsilon'(\omega) - \varepsilon''(\omega) = 1/j\ \omega C_0 Z^* \quad (8)$$

where the energy stored and lost during each cycle of the applied electric field is represented by the real ε'(ω) and imaginary ε''(ω) components (Woo *et al*., 2012). Impedance measurements were performed at frequencies ranging from 0.1 Hz to 1 MHz, and it was found that the dielectric constant decreased steadily in the low-frequency region, ranging from 0.1 to 10000 Hz, and remained constant from this point onwards in the higher frequency region. Owing to the free charge mobility inside the material, the dielectric constant is relatively high at lower frequencies (Ladhar *et al*., 2015). Higher values were accounted for by the existence of space charge effects, which resulted from charge carrier building close to the electrodes. It was found that the dielectric constant ε' is largely frequency-independent at higher frequencies. In the high-frequency range $10^4$ – $10^6$ Hz, ε' and ε" for different concentrations followed the same sequence as the ionic conductivity. Sample CA 1 M showed the highest value followed by CA 0.67 M, 0.5 M, and 0.3 M. Celgard 1 M was also positioned between CA 0.5 M and 0.67 M. Dynamics of the ε' and ε" for the whole frequency range also exhibited similar order to the conductance spectra (Figure 4(a)), as shown in Figure 5 (a), and (c), respectively.

A low frequency provides greater dielectric loss, which is followed by a reduction in ε" as the frequency increases. The collision of the mobile charge carriers causes apparent heat dissipation in the system and dielectric loss. A noticeable relaxation peak can be observed in the dielectric loss curves on the higher frequency side. Side-group dipoles may be the reason for this (Rajeswari *et al*., 2014; Zhu, 2014).

### *3.5 Loss tangent*

The loss tangent plot, shown in Figure 6, is a function of the loss tangent versus frequency plot. The ratio of the imaginary to real portion of permittivity, or the ratio of energy lost to energy retained (ε″/ ε'), is known as the loss tangent (tan δ). It starts off low in the low-frequency region, steadily increases, and reaches

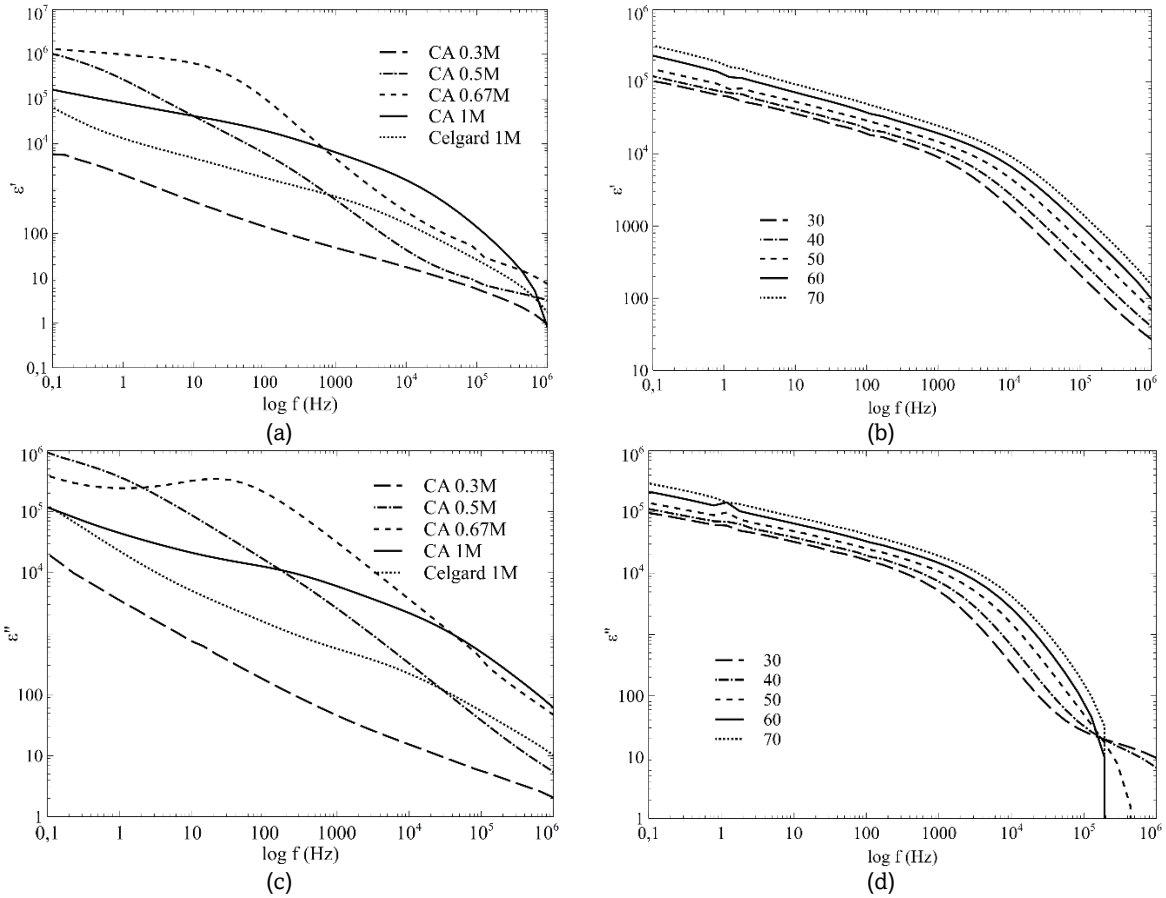


**Fig 5.** Frequency dependent (a, b) dielectric constant and (c, d) dielectric loss of of CA SPEs at different concentration and temperature

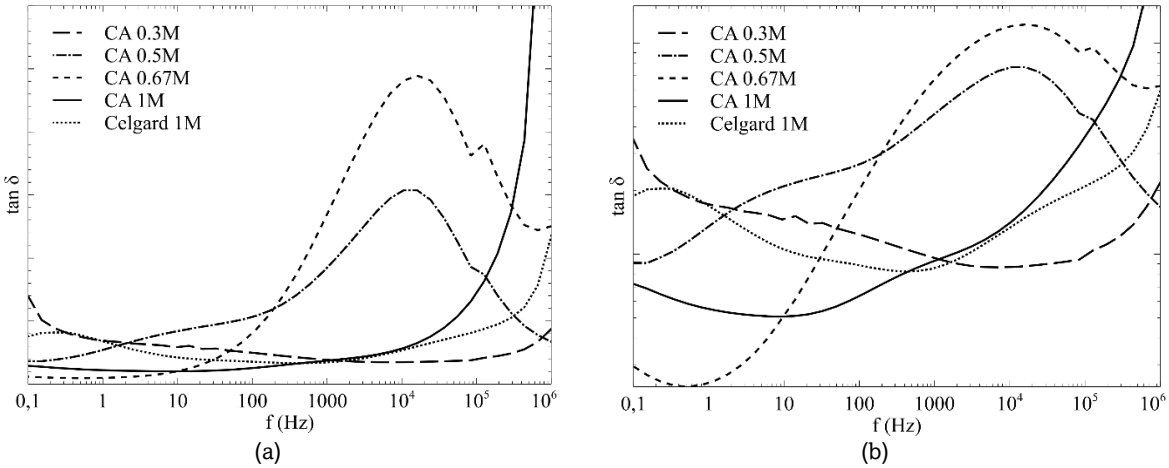


**Fig 6.** Loss tangent of (a) normal, and (b) log-log plot of CA SPEs

a maximum at a given frequency, followed by a reduction in the high-frequency region, indicating a relaxation process. The magnitude and frequency of the relaxation phenomenon would depend on the intrinsic properties of the polymer electrolyte complex (Ramesh *et al*., 2011).

It can be observed that a higher salt concentration results in a maximum shift in the loss tangent. This trend is found to be obvious for sample CA 0.5 M and 0.67 M, while for the rest of the samples it seems like the peaks are generated outside of the experiment's frequency range. The relaxation peak shifts toward the high-frequency region, indicating that ion dynamics between coordinating sites occur more quickly as a result of a reduction in relaxation time (Dieterich & Maass, 2002).

### *3.6 Modulus spectra*

The complex electric modulus was proposed by McCrum in 1967, analogous to the mechanical modulus of polymer viscoelastic relaxation (Fanggao *et al*., 1996). The plots of the real and loss moduli versus the applied frequency are presented

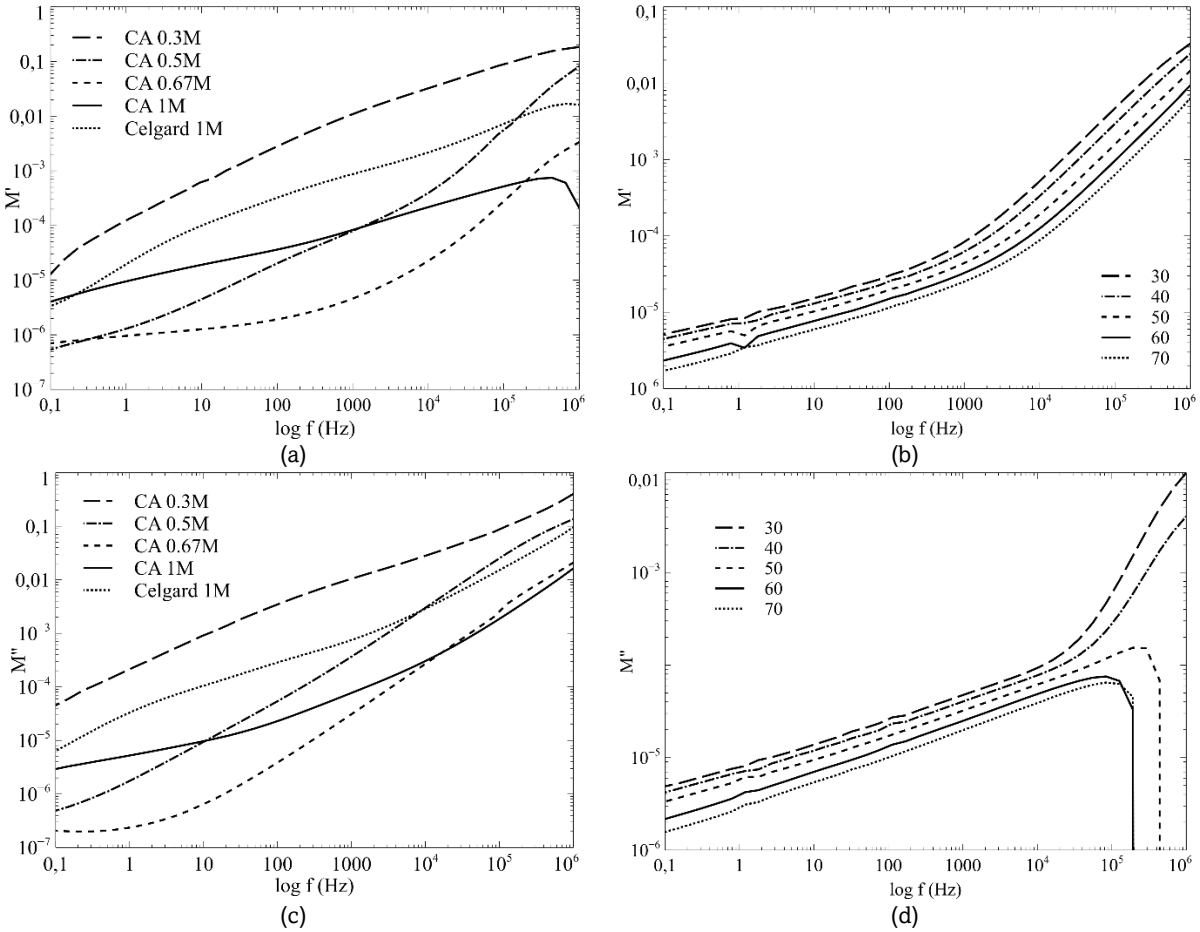


**Fig 7.** Frequency dependent of (a, b) real modulus and (c, d) loss modulus of CA SPE at different concentration and temperature

in Figure 7. The interpretation of conductivity behavior in the frequency domain can be more conveniently accomplished by utilizing the electrical modulus (M') representation. The M' model has gained significant traction in the analysis of ionic conductivities because it enables the correlation of the conductivity relaxation time with the ionic process (S. B. Aziz *et al*., 2010) . As expected, the relaxation moved from a low frequency in the permittivity spectrum to a high frequency in the modulus spectrum. Because the contribution of charge transport to the dielectric loss can be expressed as $\varepsilon'' = \sigma/\omega\varepsilon_0$, we can infer that for a given σ, ε" is higher and ω is lower. Therefore, charge accumulation close to the electrode becomes imperative in the low-frequency region, obscuring the dielectric behavior (Yusof & Kadir, 2016).

In this experiment, the modulus spectra exhibited a trend similar to that of the ionic conductivities of the samples (Figure 4). The relaxation peak appears outside the frequency range, but it can be seen that the mobility of charge carriers is enhanced at frequencies below the peak frequency, resulting in a high jump of ions at short distances (Fuqiang & Yoshimichi, 2014). The values of M' and M" are close to zero at low frequencies, indicating that the influence of the electrode polarization is insignificant and can be disregarded. The high capacitance linked to the electrodes may cause an extended tail (Ramya *et al*., 2008).

## 4. Conclusions

A polymer electrolyte membrane was successfully fabricated via a solution-casting technique using CA as the polymer host and $LiClO_4$ as the dopant salt. FT-IR spectroscopy revealed fingerprint peaks of the functional groups belonging to CA. Electrochemical impedance spectroscopy (EIS) was performed in the frequency range of 0.1 Hz to 1 MHz. Cole-Cole plot involving real and imaginary impedance axis was used to measure ionic conductivity; it was found that CA 1 M sample produces highest ionic conductivity at $3.41\times10^{-5}$ S/cm, followed by CA 0.67 M, CA 0.5 M, Celgard 1 M, and CA 0.3 M. Temperature variation is also performed within 30-70°C range. Conductance spectra revealed that the ionic conductivity of all samples decreased proportionately from high to low frequency, with a significant drop occurring at sample CA 1 M. Subsequent analysis involving the dielectric constant, loss tangent, and modulus spectra also explains that different frequency ranges exhibit different behaviors as a result of ion transport dynamics within the polymer electrolyte complex. These results provide insights into the frequency-dependent dielectric behavior and an overall justification of the performance of polymer electrolyte membranes in lithium-ion battery applications. A comparison with the Celgard© membrane as a separator in Li-ion battery systems also showed that cellulose-based polymers are a potential substitute for their petropolymer counterparts.

## Acknowledgments

This work was financially supported by a University of Indonesia Research Grant (NKB-326/UN2.RST/HKP.05.00/2022). The authors would also like to thank the Integrated Laboratory of Advanced Materials Characterization, National Research and Innovation Agency of Indonesia (BRIN), for the characterization facility.

**Author Contributions:** C.R. conceptualization, methodology, and writing. Q.S. and T.L.: Methodology, discussion, and calculations. A.F.N.: Review, editing, and project administration. S.A. and M.C.: validation and project administration. All the authors have read and agreed to the published version of the manuscript.

**Conflicts of Interest:** the authors declare no conflict of interest.

## References

Alipoori, S., Torkzadeh, M. M., Mazinani, S., Aboutalebi, S. H., & Sharif, F. (2021). Performance-tuning of PVA-based gel electrolytes by acid/PVA ratio and PVA molecular weight. *SN Applied Sciences*, 3(3), 1–13. https://doi.org/10.1007/s42452-021-04182-7

Arcana, I. M., Bundjali, B., & Hariyawati, N. K. (2014). Preparation of polymers electrolyte membranes for lithium battery from styrofoam waste. *Advanced Materials Research*, 875–877, 1529–1533. https://doi.org/10.4028/www.scientific.net/AMR.875-877.1529

Arya, A., & Sharma, A. L. (2017). Polymer electrolytes for lithium ion batteries: a critical study. *Ionics,* 23, 497–540. https://doi.org/10.1007/s11581-016-1908-6

Arya, A., & Sharma, A. L. (2018). Effect of salt concentration on dielectric properties of Li-ion conducting blend polymer electrolytes. *Journal of Materials Science: Materials in Electronics,* 29(20), 17903–17920. https://doi.org/10.1007/s10854-018-9905-3

Awang, F. F., Hassan, M. F., & Kamarudin, K. H. (2021). Corn starch doped with sodium iodate as solid polymer electrolytes for energy storage applications. *Acta Polytechnica*, 61(4), 497–503. https://doi.org/10.14311/ap.2021.61.0497

Aziz, S. B., Abidin, Z. H. Z., & Arof, A. K. (2010). Influence of silver ion reduction on electrical modulus parameters of solid polymer electrolyte based on chitosan silver triflate electrolyte membrane. *Express Polymer Letters*, 4(5), 300–310. https://doi.org/10.3144/expresspolymlett.2010.38

Aziz, Shujahadeen B., Abdullah, O. G., Rasheed, M. A., & Ahmed, H. M. (2017). Effect of high salt concentration (HSC) on structural, morphological, and electrical characteristics of chitosan based solid polymer electrolytes. *Polymers,* 9, 187. https://doi.org/10.3390/polym9060187

Chaurasia, S. K., Sharma, A. K., Singh, P. K., Lu, L., Ni, J., Savilov, S. V, Kuznetsov, A., Polu, A. R., Singh, A., & Singh, M. K. (2022). Structural, thermal, and electrochemical studies of biodegradable gel polymer electrolyte for electric double layer capacitor. *High Performance Polymers* 34(6), 1–10. https://doi.org/10.1177/09540083221101757

Das, A. M., Ali, A. A., & Hazarika, M. P. (2014). Synthesis and characterization of cellulose acetate from rice husk: Eco-friendly condition. *Carbohydrate Polymers,* 112, 342–349. https://doi.org/10.1016/j.carbpol.2014.06.006

Deng, X., Huang, Y., Song, A., Liu, B., Yin, Z., Wu, Y., Lin, Y., Wang, M., Li, X., & Cao, H. (2019). Gel polymer electrolyte with high performances based on biodegradable polymer polyvinyl alcohol composite lignocellulose. *Materials Chemistry and Physics*, 229, 232–241. https://doi.org/10.1016/j.matchemphys.2019.03.014

Dieterich, W., & Maass, P. (2002). Non-Debye relaxations in disordered ionic solids. *Chemical Physics*, 284(1–2), 439–467. https://doi.org/10.1016/S0301-0104(02)00673-0

Fanggao, C., Saunders, G. A., Lambson, E. F., Hampton, R. N., Carini, G., Di Marco, G., & Lanza, M. (1996). Temperature and frequency dependencies of the complex dielectric constant of poly(ethylene oxide) under hydrostatic pressure. *Journal of Polymer Science, Part B: Polymer Physics,* 34(3), 425–433. https://doi.org/10.1002/(SICI)1099-0488(199602)34:3<425::AID-POLB3>3.0.CO;2-S

Fernández-Sánchez, C., McNeil, C. J., & Rawson, K. (2005). Electrochemical impedance spectroscopy studies of polymer degradation: Application to biosensor development. *TrAC - Trends in Analytical Chemistry,* 24(1), 37–48. https://doi.org/10.1016/j.trac.2004.08.010

Fuqiang, T., & Yoshimichi, O. (2014). Electric Modulus Powerful Tool for Analyzing Dielectric Behavior. *IEEE Transactions on Dielectrics and Electrical Insulation,* 21(3), 929–931. https://doi.org/10.1109/TDEI.2014.004561

Galiano, F., Briceño, K., Marino, T., Molino, A., Christensen, K. V., & Figoli, A. (2018). Advances in biopolymer-based membrane preparation and applications. *Journal of Membrane Science*, 564, 562–586. https://doi.org/10.1016/j.memsci.2018.07.059

Gou, J., Liu, W., & Tang, A. (2020). A renewable gel polymer electrolyte based on the different sized carboxylated cellulose with satisfactory comprehensive performance for rechargeable lithium ion battery. *Polymer*, 208, 122943. https://doi.org/10.1016/j.polymer.2020.122943

He, R., Peng, F., Dunn, W. E., & Kyu, T. (2017). Chemical and electrochemical stability enhancement of lithium bis(oxalato)borate (LiBOB)-modified solid polymer electrolyte membrane in lithium ion half-cells. *Electrochimica Acta*, 246, 123–134. https://doi.org/10.1016/j.electacta.2017.06.043

Hu, J., Liu, Y., Zhang, M., He, J., & Ni, P. (2020). A separator based on cross-linked nano-SiO2 and cellulose acetate for lithium-ion batteries. *Electrochimica Acta*, 334. https://doi.org/10.1016/j.electacta.2019.135585

Karan, N. K., Pradhan, O. K., Thomas, R., Natesan, B., & Katiyar, R. S. (2008). Solid polymer electrolytes based on polyethylene oxide and lithium trifluoro- Methane sulfonate (PEO-LiCF3so3): Ionic conductivity and dielectric relaxation. *Solid State Ionics*, 179(19–20), 689–696. https://doi.org/10.1016/j.ssi.2008.04.034

Karthik, S., Suresh, J., Vakees, E., Kayalvizhi, M., Thangaraj, V., Balaji, K., Selvasekarapandian, S., & Arun, A. (2016). Polyvinyl Alcohol Based Solid Electrolyte Film: Synthesis, Characterization and Electrical Properties. *Macromolecular Symposia*, 362(1), 18–25. https://doi.org/10.1002/masy.201400230

Karthika, P., Sasikala, V., & Sundaresan, B. (2017). Analysis of conductance spectra and tranference number measurements on polyvinyl chloride – ammonium thio cyanate polymer electrolyte added with $SRTiO_3$ Shanlax *International Journal of Arts , Science & Humanities*. 5(1), 347–351. https://shanlax.com/wp-content/uploads/SIJ_ASH_Sep2017_V5_S1_058.pdf

Ladhar, A., Arous, M., Kaddami, H., Raihane, M., Kallel, A., Graça, M. P. F., & Costa, L. C. (2015). Ionic hopping conductivity in potential batteries separator based on natural rubber-nanocellulose green nanocomposites. *Journal of Molecular Liquids,* 211, 792–802. https://doi.org/10.1016/j.molliq.2015.08.014

Lizundia, E., Costa, C. M., Alves, R., & Lanceros-Méndez, S. (2020). Cellulose and its derivatives for lithium ion battery separators: A review on the processing methods and properties. *Carbohydrate Polymer Technologies and Applications,* 1(June), 100001. https://doi.org/10.1016/j.carpta.2020.100001

Maia, B. A., Magalhães, N., Cunha, E., Braga, M. H., Santos, R. M., & Correia, N. (2022). Designing Versatile Polymers for Lithium-Ion Battery Applications: A Review. *Polymers,* 14(3). https://doi.org/10.3390/polym14030403

Malathi, J., Kumaravadivel, M., Brahmanandhan, G. M., Hema, M., Baskaran, R., & Selvasekarapandian, S. (2010). Structural, thermal and electrical properties of PVA-LiCF3SO3 polymer electrolyte. *Journal of Non-Crystalline Solids,* 356(43), 2277–2281. https://doi.org/10.1016/j.jnoncrysol.2010.08.011

Monisha, S., Selvasekarapandian, S., Mathavan, T., Milton Franklin Benial, A., Manoharan, S., & Karthikeyan, S. (2016). Preparation and characterization of biopolymer electrolyte based on cellulose acetate for potential applications in energy storage devices. *Journal of Materials Science: Materials in Electronics*, 27(9), 9314–9324. https://doi.org/10.1007/s10854-016-4971-x

Polu, A. R., Kumar, R., & Rhee, H. W. (2015). Magnesium ion conducting solid polymer blend electrolyte based on biodegradable polymers and application in solid-state batteries. *Ionics,* 21(1), 125–132. https://doi.org/10.1007/s11581-014-1174-4

Rajeswari, N., Selvasekarapandian, S., Sanjeeviraja, C., Kawamura, J., & Asath Bahadur, S. (2014). A study on polymer blend electrolyte based on PVA/PVP with proton salt. *Polymer Bulletin*, 71(5), 1061–1080. https://doi.org/10.1007/s00289-014-1111-8

Ramesh, S., Liew, C. W., & Arof, A. K. (2011). Ion conducting corn starch biopolymer electrolytes doped with ionic liquid 1-butyl-3-methylimidazolium hexafluorophosphate. *Journal of Non-Crystalline Solids*, 357(21), 3654–3660. https://doi.org/10.1016/j.jnoncrysol.2011.06.030

Ramesh, S., Shanti, R., & Morris, E. (2013). Employment of [Amim] Cl in the effort to upgrade the properties of cellulose acetate based polymer electrolytes. *Cellulose*, 20(3), 1377–1389. https://doi.org/10.1007/s10570-013-9919-1

Ramya, C. S., Selvasekarapandian, S., Hirankumar, G., Savitha, T., & Angelo, P. C. (2008). Investigation on dielectric relaxations of PVP-NH4SCN polymer electrolyte. *Journal of Non-Crystalline Solids,* 354(14), 1494–1502. https://doi.org/10.1016/j.jnoncrysol.2007.08.038

Razalli, S. M. M., Saaid, S. I. Y. S. M., Ali, A. M. M., Hassan, O. H., & Yahya, M. Z. A. (2015). Cellulose acetate-lithium bis(trifluoromethanesulfonyl)imide solid polymer electrolyte: ATR-FTIR and ionic conductivity behavior. *Functional Materials Letters,* 8(3), 3–6. https://doi.org/10.1142/S1793604715400172

Sampath, U. G. T. M., Ching, Y. C., Chuah, C. H., Sabariah, J. J., & Lin, P. C. (2016). Fabrication of porous materials from natural/synthetic biopolymers and their composites. *Materials,* 9(12), 1–32. https://doi.org/10.3390/ma9120991

Sudiarti, T., Wahyuningrum, D., Bundjali, B., & Made Arcana, I. (2017). Mechanical strength and ionic conductivity of polymer electrolyte membranes prepared from cellulose acetate-lithium perchlorate. *IOP Conference Series: Materials Science and Engineering,* 223(1). https://doi.org/10.1088/1757-899X/223/1/012052

Tamilselvi, P., & Hema, M. (2014). Conductivity studies of LiCF3SO3 doped PVA: PVdF blend polymer electrolyte. *Physica B: Condensed Matter,* 437, 53–57. https://doi.org/10.1016/j.physb.2013.12.028

Wang, H. H., Jung, J. T., Kim, J. F., Kim, S., Drioli, E., & Lee, Y. M. (2019). A novel green solvent alternative for polymeric membrane preparation via nonsolvent-induced phase separation (NIPS). *Journal of Membrane Science*, 574, 44–54. https://doi.org/10.1016/j.memsci.2018.12.051

Woo, H. J., Majid, S. R., & Arof, A. K. (2012). Dielectric properties and morphology of polymer electrolyte based on poly(ε-caprolactone) and ammonium thiocyanate. *Materials Chemistry and Physics,* 134(2–3), 755–761. https://doi.org/10.1016/j.matchemphys.2012.03.064

Yang, L., Furczon, M. M., Xiao, A., Lucht, B. L., Zhang, Z., & Abraham, D. P. (2010). Effect of impurities and moisture on lithium bisoxalatoborate (LiBOB) electrolyte performance in lithium-ion cells. *Journal of Power Sources*, 195(6), 1698–1705. https://doi.org/10.1016/j.jpowsour.2009.09.056

Yusof, Y. M., & Kadir, M. F. Z. (2016). Electrochemical characterizations and the effect of glycerol in biopolymer electrolytes based on methylcellulose-potato starch blend. *Molecular Crystals and Liquid Crystals,* 627(1), 220–233. https://doi.org/10.1080/15421406.2015.1137115

Zalosh, R., Gandhi, P., & Barowy, A. (2021). Journal of Loss Prevention in the Process Industries Lithium-ion energy storage battery explosion incidents. *Journal of Loss Prevention in the Process Industries,* 72, 104560. https://doi.org/10.1016/j.jlp.2021.104560

Zhao, X., Wang, W., Huang, C., Luo, L., Deng, Z., Guo, W., Xu, J., & Meng, Z. (2021). A novel cellulose membrane from cattail fibers as separator for Li-ion batteries. *Cellulose,* 28(14), 9309–9321. https://doi.org/10.1007/s10570-021-04110-3

Zhao, Y., Bai, Y., Bai, Y., An, M., Chen, G., & Li, W. (2018). A rational design of solid polymer electrolyte with high salt concentration for lithium battery. *Journal of Power Sources,* 407(July), 23–30. https://doi.org/10.1016/j.jpowsour.2018.10.045

Zhu, L. (2014). Exploring strategies for high dielectric constant and low loss polymer dielectrics. *Journal of Physical Chemistry Letters,* 5(21), 3677–3687. https://doi.org/10.1021/jz501831q